

The effect of the viscosity of epoxy prepolymer on the generated morphology in rubber-toughened epoxy resin

Sang Cheol Kim, Moon Bae Ko and Won Ho Jo*

Department of Fiber and Polymer Science, Seoul National University, Seoul 151-742, Korea

(Received 3 October 1994)

The effect of the viscosity of the epoxy prepolymer on the generated morphology in a rubber-toughened epoxy system was investigated as a function of the molecular weight of the epoxy prepolymer and the curing temperature. The formulations were composed of diglycidyl ether of bisphenol A and 4,4'-diaminodiphenylsulfone, in the presence of esterified carboxy-terminated butadiene-acrylonitrile random copolymer. The cure reaction was described by an autocatalytic reaction mechanism. Parameters describing the generated morphology, i.e. average diameter of particles, volume fraction of dispersed phase and concentration of dispersed-phase particles, were determined from scanning electron microscope observations. It was observed that the morphology changes from a bimodal to a unimodal distribution with curing temperature. This phenomenon was schematically explained by the location of the trajectory that the evolving matrix composition follows through the metastable region.

(Keywords: morphology; rubber-toughened epoxy; autocatalytic mechanism)

INTRODUCTION

The mechanical properties of rubber-toughened epoxy resin depend on the morphology developed during the phase separation process, including the total rubber content^{1,2}, the volume fraction of the rubber phase³, and the domain size and its distribution³. In the early days, several studies^{4,5} suggested that particle size may influence the extent and type of toughening mechanism, and so affect the measured toughness. Later, other studies showed that the interparticle distance, which could alter the overlapping stress fields between particles, is the single parameter determining whether a blend will be tough or brittle for pseudo-ductile matrices^{6,7}. Another study³ reported that the bimodal distribution of particle sizes appears to give a definite advantage compared to the unimodal distribution. Therefore, it is very important to control the domain size and its distribution when studying the mechanical properties of rubber-toughened epoxy resin. The domain size and its distribution are largely influenced by both formulation and curing conditions.

For rubber-toughened epoxy resins, phase separation occurs during the cure. The phase separation process will be described in this study by a nucleation-growth mechanism, since the morphologies of rubber-toughened epoxy resins are usually described as spherical domains dispersed in a continuous matrix. Williams *et al.*^{8,9} have developed a model to predict the fraction, composition,

particle size and its distribution of the dispersed phase segregated during a thermoset polymerization. The model can quantitatively explain the situation whether the system separates into two-phase morphology via nucleation-growth mechanism or spinodal decomposition.

On the other hand, the conditions under which spinodal decomposition occurs have been discussed. Recently, Yamanaka *et al.*^{10,11} have stated that the nucleation-growth mechanism is not expected to take place in any case because nucleation is recognized as a very slow process. The spherical domain structure is systematically represented as arising from the evolution of an initial co-continuous structure, although no direct experimental evidence of this model could be obtained.

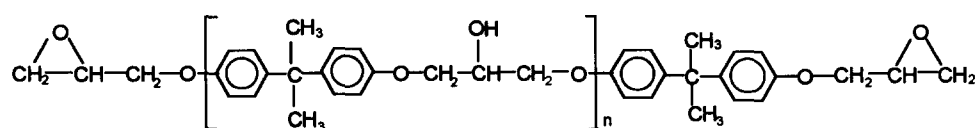
In this paper, it is our primary objective to investigate the effect of the viscosity of the epoxy prepolymer on the generated morphology in a rubber-toughened epoxy resin. The viscosity of epoxy prepolymer is controlled by varying the molecular weight of epoxy prepolymer and the curing temperature. The observed morphological parameters are also compared with the phase separation model recently developed in our laboratory¹².

EXPERIMENTAL

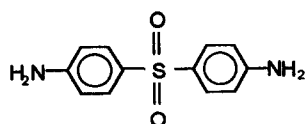
Materials

The epoxy used in this study was a commercial diglycidyl ether of bisphenol A (DGEBA), provided by KukDo Co. Two liquid types, medium-viscosity and high-viscosity epoxy resins, and one solid type were selected. The characteristics of each one are listed in

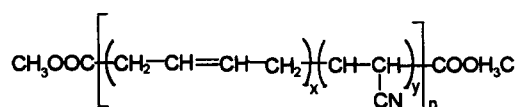
* To whom correspondence should be addressed



Diglycidyl ether of bisphenol A (DGEBA)



4,4'-Diamino diphenylsulfone (DDS)



α,ω -Methyl carboxylate butadiene-acrylonitrile copolymer (est-CTBN)

Figure 1 Chemical structure of materials used in the preparation of rubber-modified epoxy resin

Table 1 Characteristics of epoxy resins

	Epoxy equivalent weight	Relative density
YD-128 ^a	184–190	1.17
YD-134 ^b	230–270	1.18
YD-011 ^c	450–500	1.16–1.20

^a Medium-viscosity liquid type

^b High-viscosity liquid type

^c Solid type

Table 1. The curing agent was 4,4'-diaminodiphenylsulfone (DDS, Aldrich Co.). It is a crystalline solid with a relative molecular mass of 248.3, a functionality of 4 and a melting point of 176°C. A random copolymer of butadiene and acrylonitrile (27%) terminated with carboxyl groups (Hycar CTBN1300X13, B. F. Goodrich Co.) was used as a rubber modifier. Its number-average molar mass was ca. 3700 g mol⁻¹, and its relative density and carboxyl group content were 0.960 (at 25°C) and 2.4%, respectively. The chemical structure of each component is shown in Figure 1.

For a simple comparison of experimental data with a thermodynamic model, the terminated carboxyl group was substituted by methyl ester, which prevents the reaction between epoxy and rubber. The term 'est-CTBN' refers to α,ω -methyl carboxylate butadiene-acrylonitrile copolymers. The methyl esters of the carboxy-terminated copolymers were prepared by refluxing the copolymer in methanol for 9 h.

Formulations

The curing agents of 33.2, 24.8 and 13.1 phr were mixed with YD-128, YD-134 and YD-011 epoxy resins, respectively, to yield the stoichiometric mixtures for those

systems. Then 5 wt% est-CTBN was added. Each formulation was dissolved in 1:10 (w/v) ratio in methyl ethyl ketone at room temperature. Solvent was evaporated in a convection oven at 75°C for 4 h, and the residual solvent was removed under vacuum at 50°C. Hereafter, the three formulations used in this study will be referred to as YD-128, YD-134 and YD-011, as named after epoxy resins. In order to observe the morphological change with curing temperature, each formulation was cast into an aluminium dish and then cured at three different temperatures 100, 140 and 180°C for 6, 12 and 24 h. The cured resins were fractured in liquid nitrogen, and the rubber was extracted with tetrahydrofuran. The fractured surfaces were observed using a scanning electron microscope (XL, Philips Co.), after being coated with a gold sputter in vacuum.

Measurements

The cure kinetics of epoxy resins were determined by differential scanning calorimetry (d.s.c., Perkin-Elmer DSC-7). The d.s.c. was calibrated with high-purity indium and the baseline was established using two empty sample pans. For isothermal experiments, the instrument was first equilibrated at a desired temperature before the sample pan was inserted. The sample reaches thermal equilibrium within 1–2 min after the insertion of the sample pan. The exothermic reaction was considered to be complete when the rate curve levelled off to the initial isothermal baseline. Samples were scanned from 30 to 300°C at heating rates of 6, 8, 10 and 12°C min⁻¹, and the maximum heat was taken to represent the ultimate heat of cure (H_{ult}).

The viscosity was monitored with Rheometrics mechanical spectrometer (RMS 800) equipped with a modified parallel plate. The frequency of 6.28 rad s⁻¹ was selected through all measurements.

RESULTS AND DISCUSSION

Cure kinetics

The uncatalysed reaction of an epoxy resin with a primary amine produces a secondary amine, and the secondary amine subsequently reacts with another epoxide group to yield a tertiary amine. These reactions are catalysed by the hydroxyl groups that are produced during cure. Epoxy-amine systems show that the initial reaction rate has a non-zero value, and the reaction rate shows a maximum. Such behaviour is characteristic of chemical reactions in which the product itself acts as a catalyst for the reaction, a so-called autocatalytic reaction.

The heat released during cure, measured as a function of time and temperature, was assumed to be directly proportional to the rate of cure ($\dot{\alpha}$):

$$\dot{\alpha} = \frac{d\alpha}{dt} = \frac{1}{H_{ult}} \frac{dH}{dt} \quad (1)$$

where H_{ult} is the ultimate heat of cure. The extent of cure (α) was taken as the heat evolved at a certain time (H_t) divided by the total heat of cure (H_{ult}):

$$\alpha = \frac{H_t}{H_{ult}} \quad (2)$$

The curing reaction of epoxy-amine systems can be described by the following kinetic expression¹³⁻¹⁵:

$$\dot{\alpha} = \frac{d\alpha}{dt} = (K_1 + K_2 \alpha^m)(1 - \alpha)^n \quad (3)$$

where K_1 and K_2 are kinetic rate constants, and m and n are kinetic exponents. It is known that the reaction kinetics for the epoxy-amine system can be accurately described by a second-order kinetic expression, irrespective of temperature; $m + n = 2$. At the onset of the cure reaction, $t = 0$ and $\alpha = 0$, equation (3) simplifies to equation (4):

$$\left(\frac{d\alpha}{dt}\right)_{t=0} = K_1 \quad (4)$$

Therefore, K_1 can be obtained directly from the isothermal reaction rate curve. The rate constant K_2 and the kinetic exponents m and n were determined by fitting the experimental data to equation (3) using a non-linear least-squares technique.

The complete or ultimate heat of cure (H_{ult}) for the YD-128/DDS system was found to be 24.8 kcal/eq. This value agrees well with other values reported for the epoxy-amine system by Horie *et al.*¹³, Sourour and Kamal¹⁴, Riccardi *et al.*¹⁶ and Klute and Viehmann¹⁷. The values for YD-134 and YD-011 were also determined in the same way, being equal to 22.29 and 17.89 kcal/eq, respectively. Those values are much less than that for YD-128, because of their higher epoxy equivalent weights.

The temperature dependence of K_1 for each formulation is depicted in Figure 2. Slight fluctuations in determination of the onset of reactions may be responsible for the observed deviations from the Arrhenius expression. It is noted that YD-128 has the highest value of K_1 at a given temperature. This is probably due to the fact that the lower viscosity of YD-128 at an initial state as shown in Figure 3 makes the curing reactions faster. Figure 4 shows the variation of K_2 with the reciprocal absolute

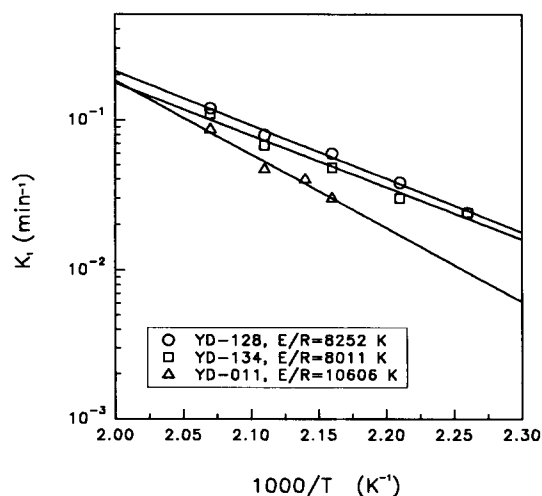


Figure 2 Kinetic rate constant (K_1) as a function of the reciprocal absolute temperature

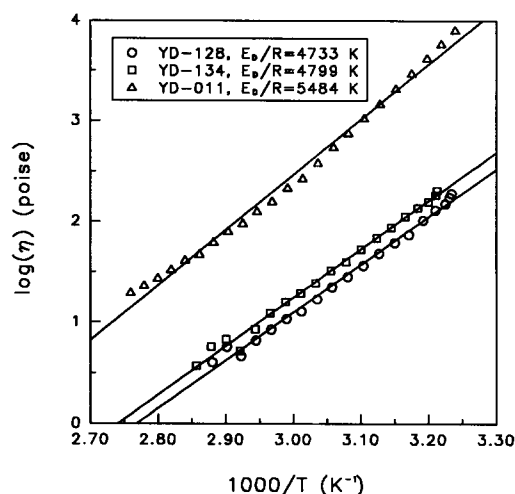


Figure 3 An Arrhenius plot of the viscosity of epoxy resins against the reciprocal absolute temperature

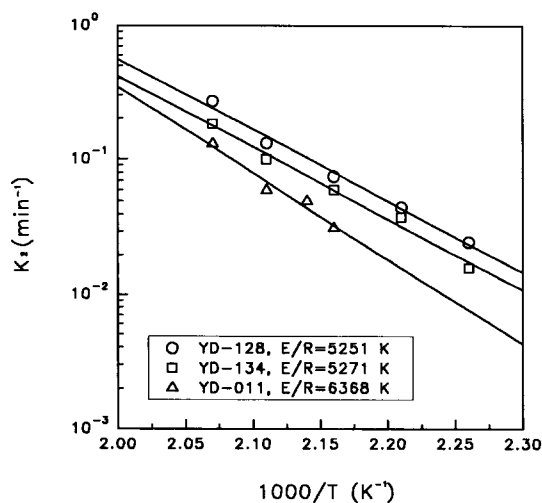


Figure 4 Kinetic rate constant (K_2) as a function of the reciprocal absolute temperature

temperature. The kinetic exponent (m) represents a quantitative measure of how much of the curing reactions follow the autocatalytic path. The values of m were found to be inversely proportional to the curing temperature for YD-128 as follows:

$$m = 2.25 - 3.78 \times 10^{-3} T \quad (5)$$

Therefore, it may be concluded that an autocatalytic reaction mechanism changes to an n th-order reaction mechanism as the curing temperature increases.

Morphological analysis

Figure 5 shows the SEM micrographs of each formulation at three different temperatures. It is observed that spherical domains are uniformly distributed in the matrix. Micrographs were magnified to calculate morphological parameters. About 500 particles of dispersed phase were analysed for each sample. The distribution of particle diameters was determined directly by measuring the diameter on the magnified SEM micrographs. The number-average diameter (\bar{D}) is defined as¹⁸:

$$\bar{D} = \frac{\sum nD}{\sum n} \quad (6)$$

where n is the number of particles having a diameter of D . The volume fraction of dispersed phase (V_D) may be calculated as:

$$V_D = \frac{\pi}{4} \left(\frac{\sum nD^2}{A_T} \right) \quad (7)$$

where A_T is the area of micrographs under analysis. Equation (7) assumes that the volume fraction is an isotropic property; hence values measured in the micrograph plane are the same as those in the real volume. This volume fraction is regarded as an effective value because it is measured in the plane of crack propagation. The concentration of dispersed particles (P) is given as:

$$P = \frac{V_D \sum n}{(\pi/6)(\sum nD^3)} \quad (8)$$

Figures 6 and 7 show the average diameter and concentration of dispersed particles as a function of the curing temperature for each formulation, respectively. The average diameter of dispersed domains shows a maximum at 140°C except YD-011, whereas the concentration of dispersed particles has a minimum value at 140°C. As discussed later, this fact suggests that the

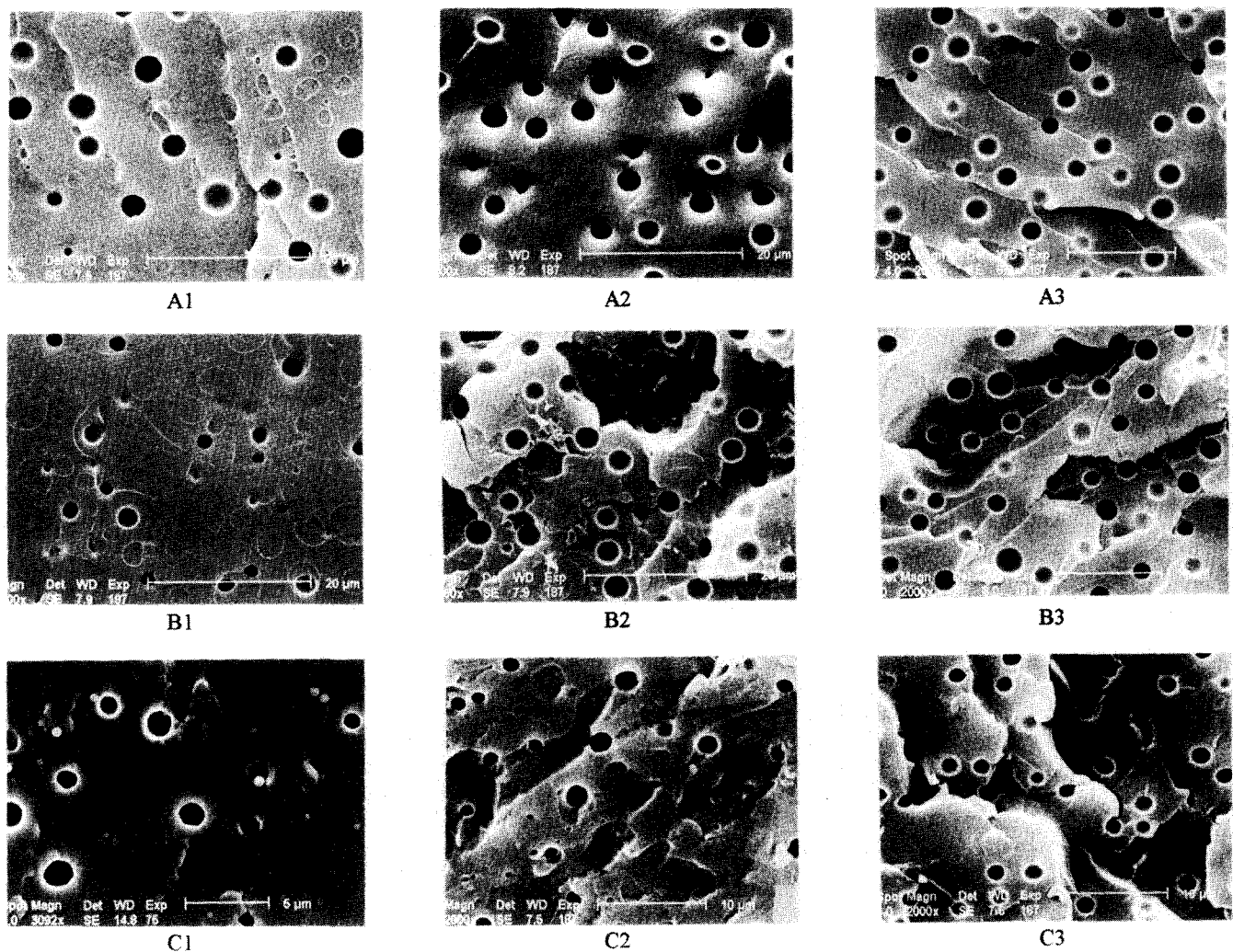


Figure 5 SEM micrographs of samples: series A, B, C denote YD-128, YD-134 and YD-011, respectively; the numbers 1, 2, 3 after A, B and C represent the curing temperature of 100, 140 and 180°C, respectively

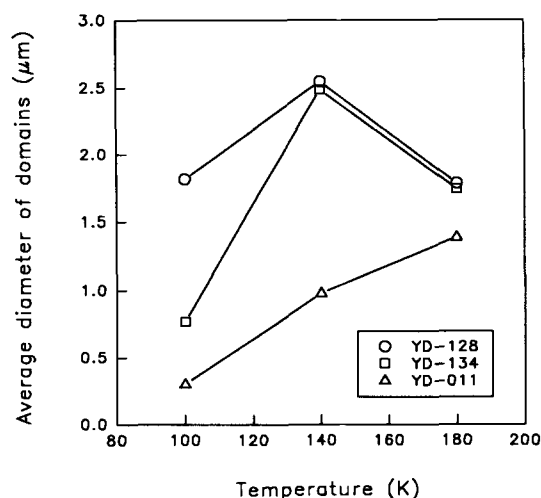


Figure 6 Plots of average diameter of domains versus the curing temperature for each type of epoxy resin

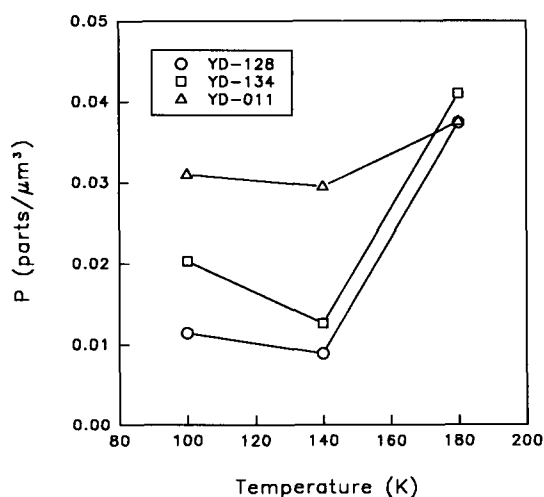


Figure 7 Plots of concentration of dispersed-phase particles (P) versus the curing temperature for each type of epoxy resin

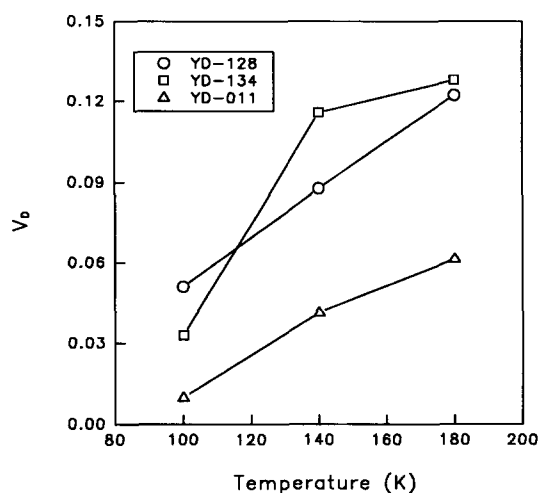


Figure 8 Plots of volume fraction of dispersed phase (V_p) versus the curing temperature for each type of epoxy resin

rate of phase separation is faster than the cure rate at a temperature lower than 140°C, but at a temperature higher than 140°C the cure rate becomes faster than the phase separation rate. Figure 8 shows that the volume fraction of dispersed domains increases with the curing temperature. As mentioned in equation (7)¹⁸, the way in which the fracture surface is produced leads to the result that the volume fraction is higher than the initial value of rubber added, 5 wt%, at high curing temperature.

Most of the morphological characteristics of rubber-modified epoxy resin depend on the location of the critical degree of cure (α_c), at which phase separation begins to take place, with respect to gel point (α_{gel}). If α_c is very close to α_{gel} , the high viscosity of the system results in a low diffusion coefficient, which will prevent significant phase separation. On the other hand, if the value of α_c is very low compared with the value of α_{gel} , the system is easily phase-separated and the low viscosity of the medium may lead to a significant coalescence of dispersed rubbery phase. Thus it is very important to control the location of α_c with respect to α_{gel} to obtain desirable morphologies. This may be achieved by two methods: first, the change of rubber nature (the increase of acrylonitrile content in CTBN) may improve the compatibility between epoxy and rubber and thus increase α_c ; secondly, the addition of chain extender may change the location of α_{gel} with respect to α_c . Once placed in the suitable operating region, the generated morphology will be determined by the trajectory that the evolution of the matrix composition follows in the metastable region. Its location will depend on the ratio of the phase separation rate to the cure rate.

Figure 9 shows the variation of particle size distribution with the curing temperature for each type of epoxy resin. The range of particle size distributions is almost the same at the three different temperatures. It is interesting to observe the following phenomenon: the distribution shows a bimodal distribution when cured at 100°C, and the larger of the two maxima is located at smaller particle size. However, the location of the larger maximum moves to larger particle size as the curing temperature increases, and finally a unimodal distribution centred at medium particle size is obtained at 180°C. This phenomenon may be schematically explained as follows. In Figure 10, ϕ_{2c} represents the actual rubber concentration in the continuous phase, and the full and dotted curves are binodal and spinodal decomposition, respectively. If phase separation proceeds much faster than the cure rate, as in the case when phase separation occurs in a low-viscosity medium (at low conversion), the trajectory of ϕ_{2c} in the metastable region will rapidly approach the bimodal curve (ϕ_2^3) owing to the high value of diffusion coefficient. When the driving force for particle growth ($\phi_2^3 - \phi_{2c}$) is small, it provokes a significant decrease in the growth rate while nucleation is still active. Consequently, the overall result is the generation of a bimodal distribution of particle sizes, as is observed at 100°C. In the temperature range of 100–140°C, the increase of the curing temperature leads to an increase in the average size of dispersed domains. This result is a general phenomenon when the morphology is controlled by the phase separation rate rather than the cure rate. On the other hand, if the cure rate is much faster than phase separation, as in the case of phase separation in a high-viscosity medium (at a high conversion), the

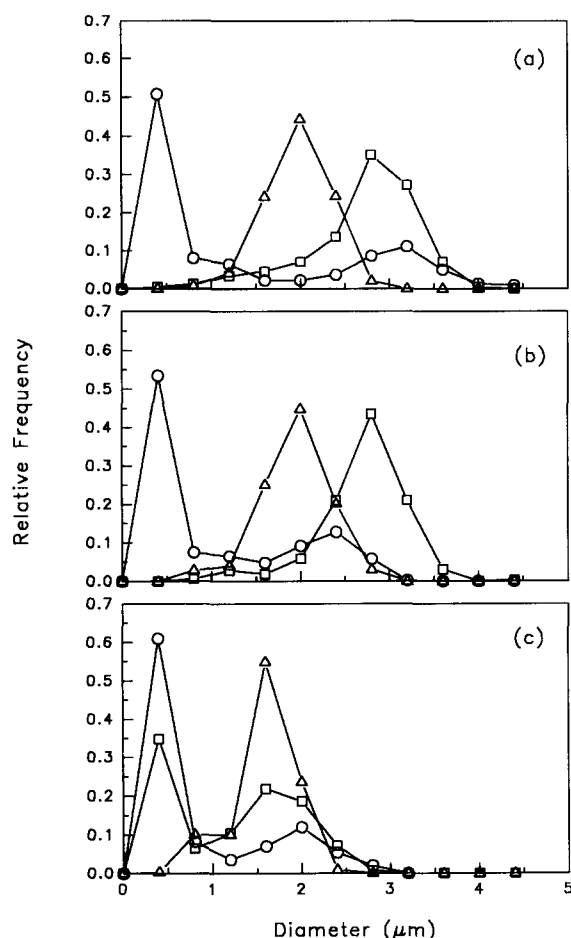


Figure 9 Particle size distribution for each type of epoxy resin: (a) YD-128; (b) YD-134; (c) YD-011. Symbols denote the curing temperature: (○) 100, (□) 140 and (△) 180 °C

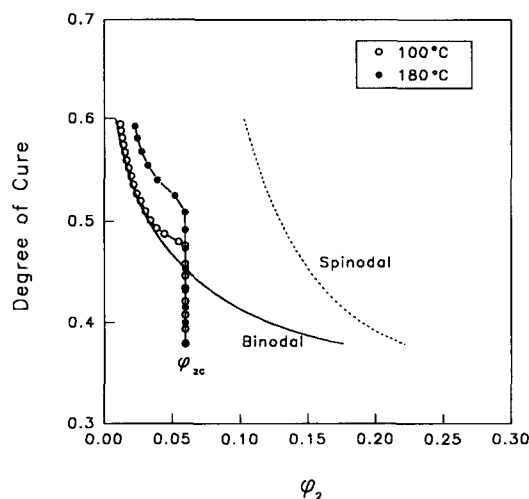


Figure 10 Comparison of trajectories in the metastable region when cured at different temperatures

trajectory of ϕ_{2c} will go up vertically to gelation owing to the low value of diffusion coefficient. Nucleation continues with the large driving force for particle growth, and the nuclei grow sufficiently until the morphology is arrested, resulting in a unimodal distribution as in the case of 180 °C.

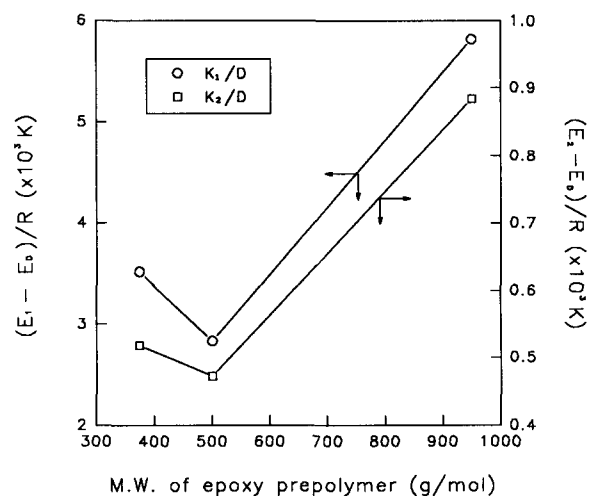


Figure 11 Difference of the activation energies between kinetic rate constant K_i and diffusion coefficient D

The change of distribution mode with temperature from bimodal to unimodal is slower in YD-011, which is still bimodal at 140 °C. The phase separation rate may be directly related to the diffusion coefficient, since both nucleation and growth rates are dependent upon the diffusion coefficient. According to the Stokes–Einstein relationship, it is inversely proportional to the viscosity as shown in Figure 3. Therefore, the ratio of the cure rate to the phase separation rate may be written as follows:

$$K_i/D \sim \exp[-(E_i - E_D)/RT] \quad (9)$$

where E_i and E_D are the activation energy for cure and diffusion, respectively. The values of E_1 , E_2 and E_D are obtained from the slopes of Figures 2, 3 and 4, respectively.

Figure 11 shows the difference of activation energies between cure and diffusion as a function of molecular weight of epoxy prepolymer. The difference of activation energies for YD-011 is larger than those for YD-128 and YD-134. This means that the cure rate for YD-011 is slower with respect to phase separation rate as compared with the others. As a result, the morphological change of YD-011 becomes relatively retarded for the same temperature jump.

CONCLUSIONS

We have investigated the viscosity effect of epoxy prepolymer on the generated morphology in a rubber-toughened epoxy resin. The viscosity of epoxy resin was controlled by varying the molecular weight of epoxy prepolymer and the curing temperature. An autocatalytic reaction mechanism of second order was used to describe the cure kinetics, and kinetic rate constants (K_1 and K_2) were determined by using a non-linear least-squares technique.

Particle size distributions were determined directly from SEM observations. An interesting observation is that the size distribution is changed from bimodal to unimodal as the curing temperature increases. This change is retarded when an epoxy prepolymer of higher molecular weight is used. According to our model¹², if the phase separation rate is faster than the cure rate, then a bimodal distribution is obtained. However, since the

increase of the curing temperature makes the cure rate faster than the phase separation rate, it leads to a unimodal distribution. The ratio of the cure rate to the phase separation rate determines the trajectory of the matrix composition, which is the most important factor to control morphology. The ratio is related to the difference of activation energies between cure and diffusion. The difference for YD-011 (epoxy prepolymer of the highest molecular weight used in this study) is larger than for the others, which means that morphological change becomes relatively slower for the same temperature jump.

REFERENCES

- 1 Manzione, L. J., Gillham, J. K. and McPherson, C. A. *J. Appl. Polym. Sci.* 1981, **26**, 907
- 2 Kunz, S. C., Sayre, J. A. and Assink, R. A. *Polymer* 1982, **23**, 1897
- 3 Kinloch, J. A. and Huston, D. C. *J. Mater. Sci. Lett.* 1986, **5**, 1207
- 4 Sultan, J. N. and McGarry, F. J. *Polym. Eng. Sci.* 1973, **13**, 29
- 5 Bascom, W. D., Ting, R. Y., Moulton, R. J., Riew, C. K. and Siebert, A. R. *J. Mater. Sci.* 1981, **16**, 2657
- 6 Wu, S. *Polymer* 1985, **26**, 1855
- 7 Raghava, R. S. *J. Polym. Sci., Polym. Phys. Edn.* 1987, **25**, 1017
- 8 Vazques, A., Rojas, A. J., Addabo, H. E., Borrajo, J. and Williams, R. J. *J. Polymer* 1987, **28**, 1156
- 9 Moschiar, S. M., Riccardi, C. C., Williams, R. J. J., Verchere, D., Sautereau, H. and Pascault, J. D. *J. Appl. Polym. Sci.* 1991, **42**, 717
- 10 Yamanaka, K. and Inoue, T. *J. Mater. Sci.* 1990, **25**, 241
- 11 Yamanaka, K., Takagi, Y. and Inoue, T. *Polymer* 1989, **60**, 1839
- 12 Ko, M. B. and Jo, W. H. manuscript in preparation
- 13 Horie, K., Hiura, H., Souvada, M., Mita, I. and Kambo, H. *J. Polym. Sci., Polym. Chem. Edn.* 1970, **8**, 1357
- 14 Sourour, S. and Kamal, M. R. *Thermochim. Acta* 1976, **14**, 41
- 15 Ryan, M. E. and Dutta, A. *Polymer* 1979, **20**, 203
- 16 Riccardi, C. C., Addabo, H. E. and Williams, R. J. J. *J. Appl. Polym. Sci.* 1984, **29**, 2418
- 17 Klute, C. H. and Viehmann, W. *J. Appl. Polym. Sci.* 1961, **5**, 86
- 18 Verchere, D., Pascault, J. D., Sautereau, H., Moschiar, S. M., Riccardi, C. C. and Williams, R. J. J. *J. Appl. Polym. Sci.* 1991, **42**, 701